Structural optimization of a composite launch tube of man portable air defense system

Efecan Yar
Department of Mechanical Engineering, TOBB University of Economics and Technology, Ankara, Turkey and
Department of Tactical Missile Systems, Roketsan Missiles Industries Inc, Ankara, Turkey, and
Erdem Acar
Department of Mechanical Engineering, TOBB University of Economics and Technology, Ankara, Turkey

Abstract

Purpose – The purpose of this paper is to find the optimum configuration of the composite launch tube currently being developed in Roketsan. The winding thicknesses and winding angles of the launch tube are selected as design variables, and three different composite material alternatives are evaluated: glass/epoxy, carbon/epoxy and aramid/epoxy.

Design/methodology/approach – In this study, structural optimization of a composite launch tube of man portable air defense system is conducted. To achieve a cost-effective design, a cost scoring table that includes structural weight, material cost, availability and manufacturability is first introduced. Then, optimization for minimum weight is conducted, where the winding thicknesses and winding angle are taken as design variables, and the safety factor value obtained by using the Tsai–Wu damage criterion is used as constraint. A surrogate-based optimization approach is used where various options for surrogate models are evaluated. Glass/epoxy, carbon/epoxy and aramid/epoxy are considered as alternative materials for the launch tube. Finally, the selection of the most cost-effective design is performed to achieve optimum cost.

Findings – Carbon fiber-reinforced epoxy matrix material provides the optimum cost-effective design for the launch tube.

Practical implications – The findings of the paper can be used to design more cost-efficient composite launch tube currently being developed in Roketsan.

Originality/value – The existing studies are based on a design approach to achieve minimum weight of the launch tubes, whereas this study introduces a design approach to achieve optimum cost.

Keywords Optimization, Composite material, Surrogate model, Cost-effective design, Launch tube

Paper type Research paper

1. Introduction

Composite materials are used in many different sectors such as aviation, automotive, sports and biomedical. The reason why composite materials are preferred is that they show high mechanical and physical strength properties at low weights compared to many conventional materials (Elmarakbi, 2013; Brischetto, 2018; Sharma *et al.*, 2019). The use of composite materials is continuously increasing. The market volume for composite materials reached 10.4 million tons in 2015 and 10.8 million tons in 2016; market volume is expected to reach 12.9 million tons for 2021. With the market volume, the market value of composite materials also increases, and this increase is expected to continue (Holmes, 2017).

Defense industry is one of the main sectors where composite materials are frequently used. Man Portable Air Defense System (MANPADS), one of the defense industry products, is the shoulder-launched land-to-air missile system. In this system, there is a launch tube that supports the missile, performs the functions required for the safe transportation and storage of the missile, protects the missile from external influences until the moment of firing and completes its function with the firing and separation of the missile (Okpara and Bier, 2008).

Composite materials are used in the launch tube of many MANPADS to reduce the system weight and increase corrosion resistance (Akkas, 2018). For instance, glass fiber-reinforced epoxy matrix material (glass/epoxy) is used for the launch tube of the Igla Portable Air Defense System manufactured by Konstruktorskoye Byuro Mashynostroyeniya (Barrie, 2002). For the Javelin Portable Anti-Tank Weapon System manufactured by Raytheon, carbon fiber-reinforced epoxy matrix material (carbon/epoxy) is used, and for the Stinger Portable Air Defense System, also manufactured by Raytheon, an aramid fiber reinforced epoxy matrix material (aramid/epoxy) launch tube is used (Simon, 2006).

The existing studies on structural optimization of launch tubes are often based on design approach to achieve minimum weight (Wang *et al.*, 1999; Atar and Acar, 2015; Davis, 2015; Akkas, 2018); however, this study introduces a design approach

The current issue and full text archive of this journal is available on Emerald Insight at: **https://www.emerald.com/insight/1748-8842.htm**

Aircraft Engineering and Aerospace Technology
93/5 (2021) 809–820
 [ISSN 1748-8842]
[DOI 10.1108/AEAT-01-2021-0002]

Funding provided by Roketsan Missiles Industries Inc. is greatly acknowledged.

Received 8 January 2021
Revised 30 March 2021
Accepted 13 April 2021

to achieve optimum cost. In structural optimization, surrogate models are widely used to reduce the computational cost. Surrogate models mimic the behavior of the simulation model (e.g. finite element model) as closely as possible while being computationally more efficient to evaluate. Commonly used surrogate models include response surface approximations (Myers and Montgomery, 1995), radial basis functions (Buhmann, 2003), Kriging (Acar, 2013), nonparametric regression (Hardle, 1990) and neural networks (Bishop, 1995). An extensive review of surrogate modelling techniques in support of engineering design optimization can be found in Queipo *et al.* (2005). The latest and significant studies on surrogate based optimization include Hao *et al.* (2018, 2020) and Fernández-Godino *et al.* (2019).

The objective of this paper is to find the optimum configuration of the composite launch tube currently being developed in Roketsan. The winding thicknesses and winding angles of the launch tube are selected as design variables, and three different composite material alternatives are evaluated: glass/epoxy, carbon/epoxy and aramid/epoxy. The selection of the optimum design configuration is based on a cost scoring that includes structural weight, material cost, availability and manufacturability.

The paper is structured as follows. In Section 2, the problem definition is given. Finite element modeling of the launch tube is discussed in Section 3. The optimum design selection criterion is given in Section 4. The results are presented in Section 5, followed by some concluding remarks given in Section 6.

2. Problem definition

In this study, winding thicknesses and winding angle of the launch tube are selected as design variables. Optimization for minimum cost requires developing a cost function in terms of the design variables for each composite material alternative, and this is an extremely challenging task. For simplification, we optimize each composite material alternative for minimum weight, and evaluate these alternative designs according to a cost scoring table that includes structural weight, material cost, availability and manufacturability. The design alternative having the smallest cost is considered to be the most cost-effective design.

2.1 Optimization for minimum weight

The optimization problem for minimum weight can be written in standard form as:

$$\begin{aligned} &\text{Find} && t_1, t_2, \theta \\ &\text{Min} && \mathrm{W}(t_1, t_2) = \left(\pi(r_i + 2.t_1 + t_2)^2.h - \pi(r_i)^2.h\right).\rho \\ &\text{S.t.} && \mathrm{SF}(t_1, t_2, \theta) \geq 3 \\ &0.1\,\text{mm} \leq t_1, t_2 \leq 2\,\text{mm} \\ &0 \leq \theta \leq 90^\circ \end{aligned} \tag{1}$$

Here, ρ refers to density of composite material (1.9, 1.6 and 1.4 g/cm^3 for glass/epoxy, carbon/epoxy and aramid/epoxy, respectively), h refers to height of the cylindrical launch tube which is 1690 mm and r_i refers to inside radius of cylindrical launch tube which is 95 mm. We consider that the launch tube is made of three layers, where t_1 and t_2 are winding thicknesses, and θ is the winding angle of the launch tube (Figure 1). The objective function is the structural weight W(t_1, t_2). In modern composite structures, winding thickness can be reduced to 0.1 millimeters (Vasiliev and Morozov, 2013). For this reason, 0.1-mm value is used as the lower bound for the winding thicknesses t_1 and t_2 in equation (1), and the upper bound of 2 mm is determined by intuition. For the composite launch tube, the safety factor (SF) is determined as 3 based on the study of Wagenen (1989).

The safety factor (SF) in equation (2) is calculated based on the Tsai–Wu failure criterion that is frequently used in analysis studies and gives values close to real results for most composite materials (Yeh *et al.*, 2009):

$$\begin{aligned} &\left(F_{11}{\sigma_1}^2 + F_{22}{\sigma_2}^2 + F_{66}{\sigma_6}^2 + 2F_{12}\sigma_1\sigma_2\right)(SF)^2 \\ &+ (F_1\sigma_1 + F_2\sigma_2)(SF) = 1 \end{aligned} \tag{2}$$

where F_{11}, F_{22}, F_{66}, F_1, F_2 ve F_{12} are strength parameters, which are calculated from:

$$F_{11} = \frac{1}{X_t X_c}, \quad F_{22} = \frac{1}{Y_t Y_c}, \quad F_{66} = \frac{1}{S^2}, \tag{3}$$

$$F_1 = \frac{1}{X_t} - \frac{1}{X_C}, \quad F_2 = \frac{1}{Y_t} - \frac{1}{Y_C}, \quad F_{12} = -\frac{1}{2}\sqrt{F_{11}F_{22}}$$

In equation (2), σ_1 value is the stress in the fiber direction, σ_2 value is the stress perpendicular to the fiber direction, σ_6 value is the shear stress. In equation (3), X_C is the compressive strength in the fiber direction, X_t is the tensile strength in the fiber direction, Y_C is the compressive strength perpendicular to the fiber direction, Y_t is the tensile stress perpendicular to the fiber direction and S value indicates the shear strength.

2.2 Cost function modeling

After the minimum weight designs are obtained for each composite material alternative, these alternative designs are evaluated according to a cost scoring that includes structural weight, material cost, availability and manufacturability. A percentage rating, presented in Table 1, is generated to evaluate the cost-effectiveness of a launch tube design. Table 1 is generated based on the current conditions and the experience of Izoreel Composites.

Availability and manufacturability scores are determined based on the feedback of Izoreel Composites, a composite material manufacturer located in İzmir, Turkey. Notice that the scores are normalized such that the highest score is 10.

Table 2 shows the availability scores of all alternatives. The most available material is glass/epoxy and the least available one

Figure 1 Layers of launch tube and winding angles

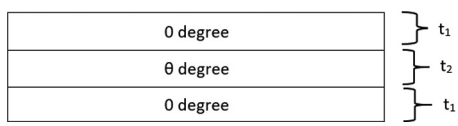

Table 1 Launch tube cost rating chart

Criteria	Percentage rating (%)
Availability	25
Manufacturability	15
Weight	45
Material cost	15
Total	100

Table 2 Availability scores

Alternatives	Comparison	Score
Glass/Epoxy	– High score due to the ease of glass fiber supply (5) – High score due to availability of alternative manufacturers (5)	10
Carbon/ Epoxy	– High score for ease of supply due to domestic production (5) – Medium score due to alternative availability of carbon fiber (3)	8
Aramid/ Epoxy	– Medium score due to the difficulty of obtaining aramid fiber (3) – Medium score due to alternative availability of aramid fiber (3)	6

is aramid/epoxy. Scoring is carried out based on the current conditions and the experience of Izoreel Composites.

Table 3 shows that glass/epoxy and carbon/epoxy have high manufacturability. However, when machining process is desired to be performed on aramid/epoxy, it is due to the fact that the fibers inside do not allow the machining method by dispersing. Different methods such as laser cutting should be used to achieve proper cutting in aramid/epoxy.

Table 4 shows approximate unit price for alternative materials (Tempelman *et al.*, 2014). When unit prices are compared, the aramid/epoxy is the most expensive among all alternatives per unit weight. The unit prices of glass/epoxy and the carbon/epoxy are found to be 0.4 times and 0.6 times that of the aramid/epoxy, respectively.

Weight score is determined as a result of weight optimization study. For material cost score, unit price and the result which is obtained by weight optimization study is necessary. Therefore, weight and material cost scores are given in the next sections.

Table 3 Manufacturability scores

Alternatives	Comparison	Score
Glass/Epoxy	High manufacturability due to the use of glass fiber	10
Carbon/ Epoxy	There are no difficulties in using carbon fiber for the launch tube subsystem, therefore high manufacturability	10
Aramid/ Epoxy	Using aramid fiber is high for fiber winding process; low manufacturability in terms of cutting and machining	7

Table 4 Unit price for alternatives

Alternatives	Approximate unit price (€/kg) [12]
Glass/Epoxy	20
Carbon/Epoxy	30
Aramid/Epoxy	50

3. Finite element modeling

In this paper, ANSYS finite element software is used to compute the structural performance of the launch tube (e.g. weight and safety factor). The geometry of the launch tube is simplified as a shell of 95 mm in diameter and 1690 mm in length. Glass/epoxy, carbon/epoxy and aramid/epoxy are selected as composite materials with properties presented in Table 5. These material properties are taken from Daniel and Ishai (2006) and MatWeb (www.matweb.com).

The composite layers are created using the ANSYS Composite PrepPost (ACP) module. In this study, three layers are created and the angle of these layers are assigned as [0, θ, 0], respectively. 0-degree angles are kept constant, whereas θ angle is used as a design variable. The winding thickness t_1 of the layers with winding angle of 0 degrees, and winding thickness t_2 of the layers with winding angle of θ degree are taken as design variables as well. After the layers of the composite model are created, the winding angle and winding thicknesses are parametrized as input, and the weight and safety factor as output in ANSYS (Figure 2).

As the coordinate axis, the x-axis shows the front part of the launch tube, that is the exit direction of the missile. The y-axis shows the lateral direction and the z-axis shows the gravity direction. The loading and boundary conditions are given in this coordinate axis. The regions indicated in Figure 3 are the regions where the displacement is zero on the x-, y- and z-axis. These regions represent the gripstock interfaces that enable the missile to be fired, and as gripstock interfaces are accepted as rigid bodies, they do not undergo deformation at the time of firing. For this reason, the regions specified in Figure 3 are accepted as the regions where the launch tube is fixed.

In Figure 4, the shoulder support of the launch tube is modeled as a pin support. As the personnel using the man-portable air defense system must keep the gripstock stationary, it is not possible for the launch tube to rotate around its own axis (x-axis). Therefore, rotational movement around the x-axis does not occur in the shoulder support region.

There is a monocular structure on the gripstock, and while searching the target, the personnel brings their eyes closer to this monocular. If the rotational movement of the system around the z-axis is released in the shoulder support region, it will be difficult for the personnel to look through the monocular. For this reason, it is more appropriate to move the whole body without turning the head. Therefore, the rotational movement around the z-axis in the area of the shoulder support does not occur.

Rotational movement around the y-axis in the shoulder support region means that the launch tube can be moved up and down, and this movement is allowed. Therefore, the rotational motion around the y-axis is released and the value zero for the other axes is taken.

Force measurements are conducted in the test area by placing two three-axis force gauges on the fixed parts of the launch tube as indicated in Figure 5. PCB brand's device with model number 261A03 is used as force gauge. The coordinate axis selected for the force gauges is the same as the coordinate

Table 5 Properties of composite materials

Material properties	Symbol	Unit	Glass/ Epoxy	Carbon/ Epoxy	Aramid/ Epoxy
Longitudinal modulus	E_1	MPa	41000	127700	83000
Transverse modulus	E_2	MPa	10400	7400	7000
Poisson's ratio	ν	–	0.28	0.33	0.41
Shear modulus in the fiber direction	G_1	MPa	4300	6900	2100
Shear modulus perpendicular to fiber direction	G_2	MPa	3500	4300	1860
Tensile strength in the fiber direction	X_t	MPa	1140	1717	1377
Tensile strength perpendicular to fiber direction	Y_t	MPa	39	30	18
Compressive strength in the fiber direction	X_c	MPa	620	1200	235
Compressive stress perpendicular to fiber direction	Y_c	MPa	128	216	53
Shear strength	S	MPa	89	33	27
Density	ρ	g/cm^3	1.9	1.6	1.4
Specific heat	c	J/kg.K	800	1000	1420
Longitudinal thermal expansion coefficient	α_1	10^{-6}/°C	7	−0.9	-2
Transverse thermal expansion coefficient	α_2	10^{-6}/°C	26	27	60

Figure 2 Inputs and outputs used in the ANSYS model

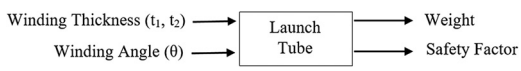

Figure 3 Regions where the launch tube is fixed

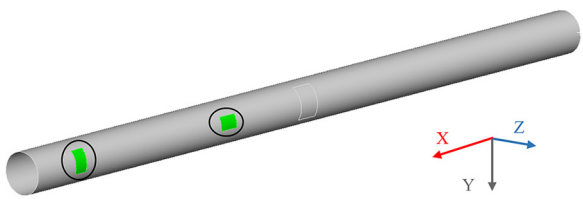

Figure 4 Section where launch tube shoulder support is provided

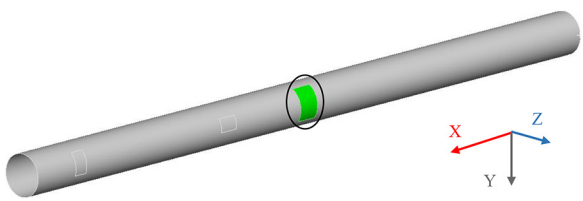

axis used in the launch tube analysis. The range of 0.75 to 1 s, when the loading is maximum, is used in the analysis, and the loads obtained from the force gauge data are averaged. Force data are graphically shown in Figure 6.

To perform thermal load analysis, thermocouples are placed in the front, middle and rear parts of the launch tube. The missile is fired in the test area, and the temperature measurement is conducted. The measurement results are graphically shown in Figure 7. It is seen that the temperature value in the launch tube is higher at the rear, because the ejection motor that provides the propulsion of the missile in the launch tube is located in the rear section. Thermal loads obtained from thermocouples are applied on the launch tube in ANSYS.

A mesh convergence study is carried out for three alternative composite materials. The shell structure is 95 mm in diameter

Figure 5 Locations of the force gauges

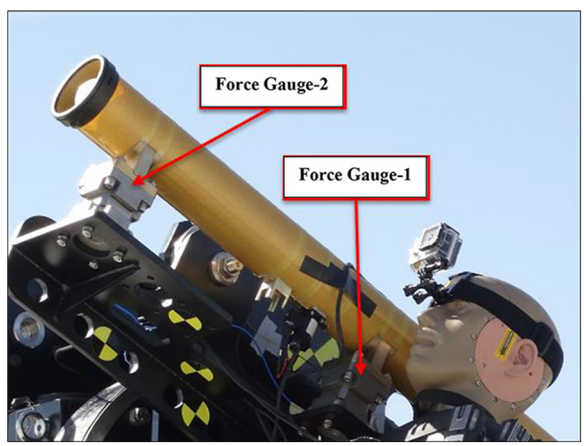

and 1690-mm high. The launch tube is defined by creating a mesh with the shell181 element. According to ANSYS documentation, shell181 is a four-node element with six degrees of freedom at each node (translations in X, Y and Z directions and rotational movement around *x*-, *y*- and *z*-axes). For mesh convergence study, t_1 and t_2 values are taken 1 mm, θ value is taken 75^0. The variation of the total displacement (a square root of the summation of the square of X, Y and Z direction) with respect to the number of elements is examined. The number of elements is varied between 856 and 7958 (that corresponds to ranging the element size from 27 to 8 mm), and it is found that the mesh convergence is achieved when 6265 elements are used (that corresponds to the element size of 9 mm) as seen in Figure 8, where the element size of 9-mm element size is represented with a red dot. By choosing 9-mm element size, it is observed that the rate of difference in displacement is approximately 2 per thousand or less for all composite materials.

In addition, an additional mesh convergence study in terms of the safety factor is given in Figure 9. It is observed that the mesh convergence studies based on displacement and safety factor yielded the same element size selection.

Figure 6 Load based on time in (a) *x*- (b) *y*- (c) *z*-axis

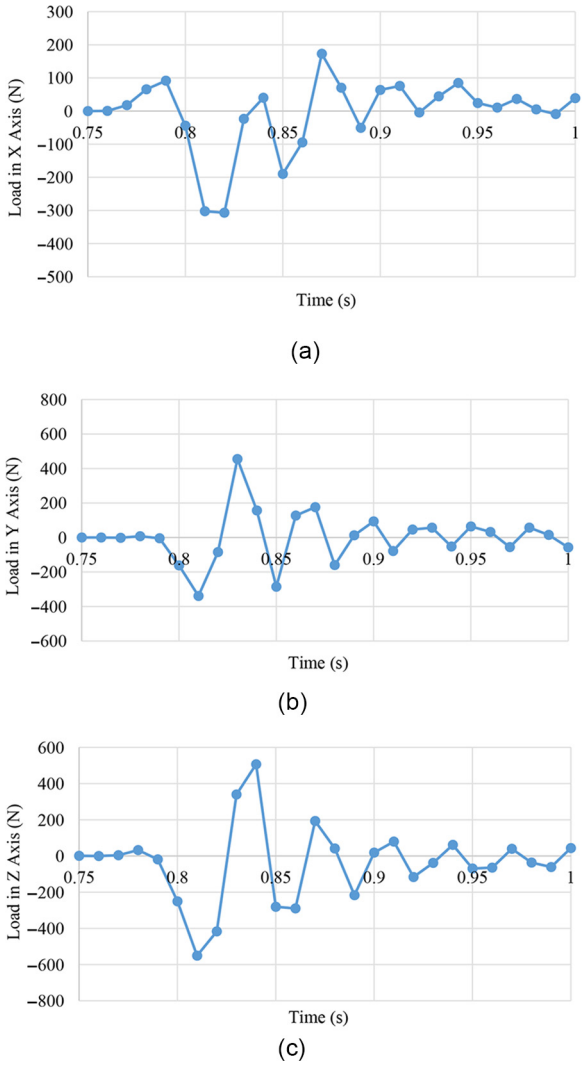

Figure 7 Temperature data taken from thermocouples on launch tube

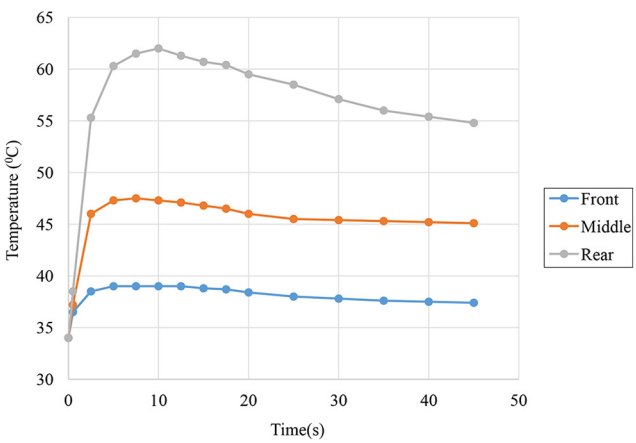

Figure 8 Mesh convergence based on total displacement for (a) glass/epoxy (b) carbon/epoxy (c) aramid/epoxy

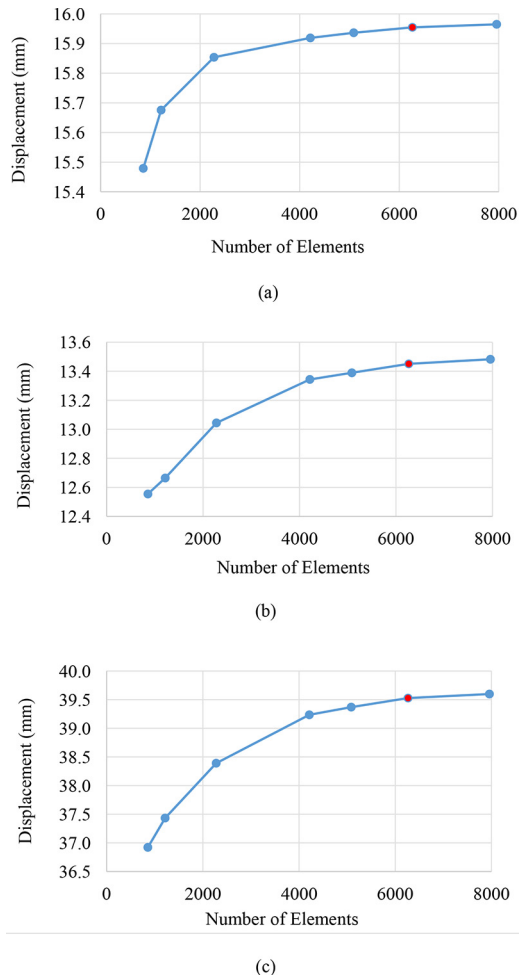

4. Results

4.1 Optimization for minimum weight

In optimization for minimum weight, a surrogate based approach is used. Figure 10 shows the flowchart of the surrogate-based optimization approach followed in this study. The optimization problem stated in equation (1) is solved by using different types of surrogate models (e.g. polynomial response surface, Kriging, non-parametric regression, genetic aggregation, neural networks), and multiple optimum candidates are obtained that correspond to each surrogate model type. Finally, the candidate having the smallest objective function is declared to be the optimum configuration. The reason for using multiple surrogate models is that the use of the most accurate surrogate model in optimization does not necessarily lead to the optimum solution, as noted earlier in various works including Glaz *et al.* (2009) and Acar *et al.* (2011).

As a first step of constructing the surrogate models, training points are generated by using Latin hypercube sampling. After the training points are generated, the corresponding response

Figure 9 Mesh convergence based on safety factor for (a) glass/epoxy (b) carbon/epoxy (c) aramid/epoxy

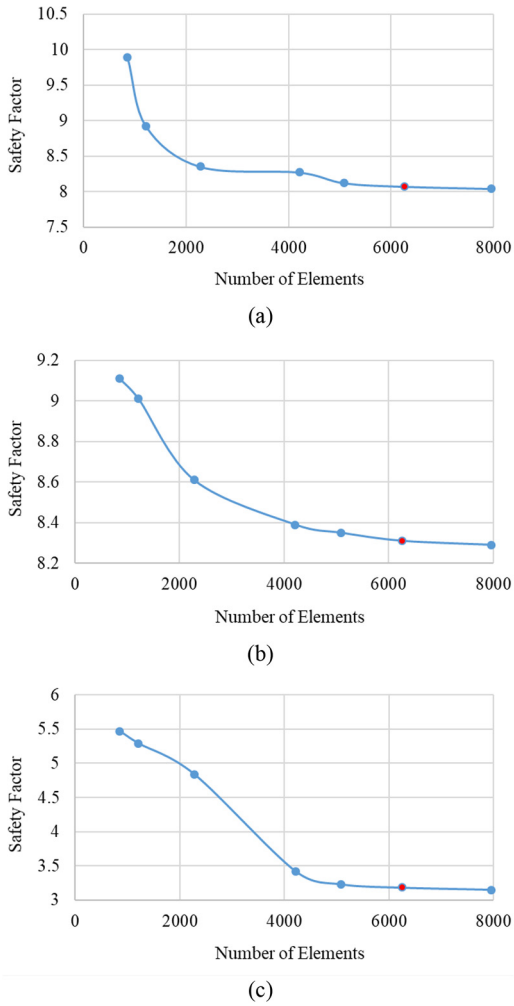

are calculated as given in Appendix 1. Then, various types of surrogate models, whose details are provided in Appendix 2, are constructed.

The accuracies of the constructed surrogate models are evaluated at some randomly selected ten test points which are provided in Appendix 3. These test points are not used in the construction of surrogate models, they are only used to evaluate the accuracy of the surrogate models. The root mean square error is selected as error metric.

Root mean square error (RMSE) is a statistical method that enables to find the distance between the predicted values and the observed values. Generally, the closer the value is to zero, the better the quality of the response surface. The square root mean error is mathematically given in equation (4):

$$RMSE = \sqrt{\frac{1}{N}\sum_{i=1}^{N}(y_i - \hat{y}_i)^2} \tag{4}$$

where N gives the number of sampling points, y_i expression gives the value of the output parameter at the ith sampling point and $\hat{y}_i$ expression gives the value of the regression model at the ith sampling point.

RMSE values for all surrogate models and for all materials are given in Table 6. It is observed that there is not much difference between the smallest and largest RMSE values of different surrogate models. For instance, for glass/epoxy material, the smallest RMSE is 1.47 whereas the largest RMSE is 2.18, and the difference between these two error values are not very large. For this reason, no surrogate model was excluded from the study and an optimization study was performed for all surrogate models.

The results obtained by using surrogate models are given in Table 7. As an optimization method, genetic algorithm is used. The default optimization algorithm parameters of ANSYS is used such that mutation probability is taken 0.01, and

Figure 10 Flowchart for surrogate-based optimization

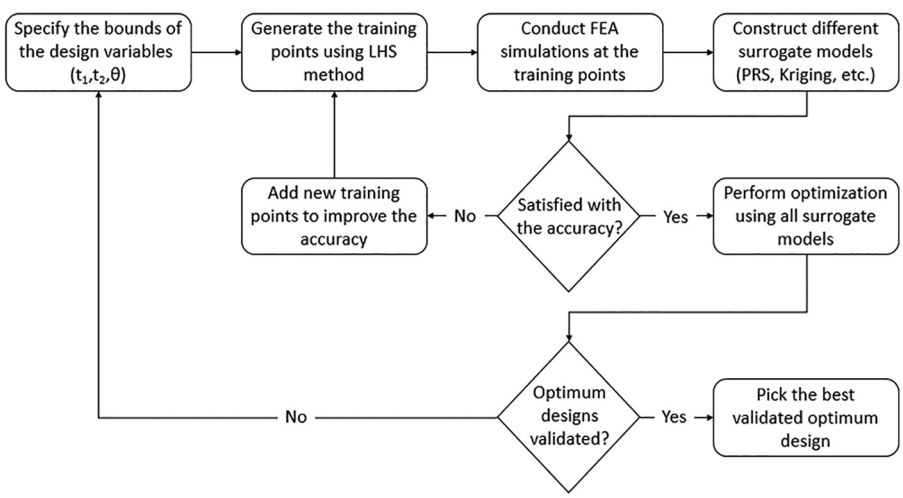

Table 6 RMSE values of the surrogate models

Surrogate model	Glass/Epoxy		Carbon/Epoxy		Aramid/Epoxy	
	SF	Weight	SF	Weight	SF	Weight
Quadratic polynomial response surface	1.57	1.14×10^{-9}	0.78	7.87×10^{-10}	1.09	*7.74×10^{-10}*
Kriging	1.53	*9.07×10^{-10}*	0.65	*5.18×10^{-10}*	0.89	9.65×10^{-10}
Nonparametric regression	*1.47*	4.95×10^{-4}	1.75	4.01×10^{-4}	1.33	5.75×10^{-4}
Genetic aggregation	1.78	1.14×10^{-9}	0.75	7.87×10^{-10}	*0.54*	*7.74×10^{-10}*
Neural network	2.18	1.22×10^{-6}	**0.55**	2.38×10^{-6}	1.59	2.04×10^{-6}

Table 7 Optimization results for minimum weight for alternative materials

Surrogate model	Quadratic polynomial response surface	Kriging	Nonparametric regression	Genetic aggregation	Neural network
Results for Glass/Epoxy Launch Tube					
θ (degree)	*87.4*	84.5	70.3	78.3	73.5
t_1 (mm)	*0.26*	0.3	0.22	0.34	0.25
t_2 (mm)	*0.76*	0.68	0.86	0.62	0.82
Safety factor	*3.08*	3.36	3.03	3.08	3.19
Weight (kg)	*1.253*	1.272	1.300	1.274	1.301
Results for Carbon/Epoxy Launch Tube					
θ (degree)	*87.8*	85.7	84.8	85.6	83.8
t_1 (mm)	*0.23*	0.37	0.3	0.21	0.16
t_2 (mm)	*0.36*	0.21	0.31	0.42	0.55
Safety factor	*3.1*	3.04	3.07	3.08	3
Weight (kg)	*0.668*	0.759	0.728	0.679	0.700
Results for Aramid/Epoxy Launch Tube					
θ (degree)	85.1	*81.7*	80.8	82.3	81.5
t_1 (mm)	0.26	*0.31*	0.32	0.42	0.18
t_2 (mm)	0.82	*0.68*	0.7	0.5	1.1
Safety factor	3.06	*3.03*	3.05	3.08	3.25
Weight (kg)	0.941	*0.915*	0.928	0.945	1.020

crossover probability is taken 0.98. The optimum launch tube weight is found to be 1.253 kg for glass/epoxy, 0.668 kg for carbon/epoxy, and 0.915 kg for aramid/epoxy. It is found that the winding angle is close to 90 degrees for all alternative materials considered in this study. It is also observed that the quadratic polynomial response surface and the Kriging methods are suitable methods to reach the lightest launch tube structure.

If the only consideration was the structural weight, then we would complete the existing study at this point by concluding that the launch tube should be designed by using carbon/epoxy material by using the winding thickness and angle values reported in Table 7. However, we have additional design considerations such as material cost, availability and manufacturability. Therefore, we continue by exploring the material cost criterion next.

4.2 Selection for cost-effective design

The unit price and the weight results are multiplied to obtain the material cost for all alternative materials. To obtain the material cost scores, the material cost values are normalized such that the highest score is 10, and it is assigned to the material with the smallest cost. Table 8 shows that the carbon/epoxy design alternative has the smallest material cost, so its material cost score is 10. The material with the next smallest cost is the glass/epoxy, and its material cost score is obtained as $20.04/25.06 \times 10 = 8.0$. Similarly, the material cost score of the aramid/epoxy is obtained as $20.04/45.75 \times 10 = 4.4$.

Table 8 Material cost scores

Alternatives	Weight (kg)	Approximate unit price (€/kg) [12]	Material cost (€)	Score
Glass/Epoxy	1.253	20	25.06	8.0
Carbon/Epoxy	0.668	30	20.04	10
Aramid/Epoxy	0.915	50	45.75	4.4

The weight scoring of different design alternatives is given in Table 9. To obtain the weight scores, the weight values are normalized such that the highest score is 10, and it is assigned

Table 9 Weight scores

Alternatives	Weight (kg)	Score
Glass/Epoxy	1.253	5.3
Carbon/Epoxy	0.668	10
Aramid/Epoxy	0.915	7.3

Table 10 Total scoring

Alternatives	Availability	Manufacturability	Material cost	Weight	Total score
Glass/Epoxy	$0.25 \times 10 = 2.5$	$0.15 \times 10 = 1.50$	$0.15 \times 8 = 1.20$	$0.45 \times 5.3 = 2.39$	7.59
Carbon/Epoxy	$0.25 \times 8 = 2.0$	$0.15 \times 10 = 1.50$	$0.15 \times 10 = 1.50$	$0.45 \times 10 = 4.50$	*9.50*
Aramid/Epoxy	$0.25 \times 6 = 1.5$	$0.15 \times 7 = 1.05$	$0.15 \times 4.4 = 0.66$	$0.45 \times 7.3 = 3.29$	6.50

to the material alternative with minimum weight. Table 9 shows that the carbon/epoxy design alternative has the smallest weight, so its weight cost score is 10. The material with the next minimum weight is the aramid/epoxy, and its weight cost score is obtained as $0.668/0.915 \times 10 = 7.3$. Similarly, the material cost score of aramid/epoxy is obtained as $0.668/1.253 \times 10 = 5.3$.

Table 10 combines all the scores related to availability, manufacturability, material cost and weight (Tables 2, 3, 8 and 9) along with Table 1 to arrive at the total score. It is seen that carbon/epoxy material has the highest score (9.50 points). It is found that the optimization for minimum weight and design selection for minimum cost resulted in the same design.

5. Concluding remarks

In this study, structural optimization of a composite launch tube of MANPADS was performed. As MANPADS are carried by the user, these systems need to be lightweight. Ply angle and ply thickness have been carefully chosen to obtain lightweight launch tube. To achieve a cost-effective design, a cost scoring table that includes structural weight, material cost, availability and manufacturability was first introduced. Glass/epoxy, carbon/epoxy and aramid/epoxy were considered as three material alternatives, and the winding thicknesses and angle of each alternative were optimized for minimum weight. Finally, these alternative designs are evaluated according to the cost scoring table. This study can be generalized by changing geometry and boundary conditions and applied to other MANPADS. From the results obtained in this study, the following conclusions were drawn:

- For glass/epoxy material alternative, the minimum weight design was achieved by using quadratic polynomial response surface and resulted in 1.253-kg design.
- For carbon/epoxy material alternative, the minimum weight design was achieved by using quadratic polynomial response surface and resulted in 0.668-kg design.
- For aramid/epoxy material alternative, the minimum weight design was achieved by using Kriging model and resulted in 0.915-kg design.
- A total score was obtained by using availability, manufacturability, material cost and weight scores, and it was observed that the use of carbon/epoxy material for the launch tube is suitable for cost effective design.

The study discussed in this paper can be extended to the following studies:

- In this study, we consider a single objective formulation for optimization. A multiobjective formulation with conflicting objectives could be considered in a future study.
- Launch tube made of a hybrid material such as a combination of carbon and glass fiber composite can be subject of a future study.
- In this study, safety factor is used as a constraint in weight optimization study. Other constraints can be added due to the complexity of the work environment. For example, a disorientation constraint can be applied in a future study for preventing crack propagation and delamination.
- In this study, the launch tube is made of three layers. As a future study, different number of plies can be considered in launch tube design.

References

Acar, E. (2013), "Effects of the correlation model, the trend model and the number of training points on the accuracy of kriging metamodels", *Expert Systems*, Vol. 30 No. 5, pp. 418-428.

Acar, E. and Rais-Rohani, M. (2009), "Ensemble of metamodels with optimized weight factors", *Structural and Multidisciplinary Optimization*, Vol. 37 No. 3, pp. 279-294.

Acar, E., Guler, M.A., Gerçeker, B., Cerit, M.E. and Bayram, B. (2011), "Multi-objective crashworthiness optimization of tapered thin-walled tubes with axisymmetric indentations", *Thin-Walled Structures*, Vol. 49 No. 1, pp. 94-105.

Akkas, O. (2018), "Design of frangible composite cover for missile launch tube", MSc thesis, Middle East Technical University, Ankara.

Atar, H. and Acar, E. (2015), "Structural optimization of payload fairing used for space launch vehicles", *Balkan Journal of Electrical and Computer Engineering*, Vol. 3 No. 4, pp. 213-219.

Barrie, D. (2002), "Russian super igla missile enters export production", *Aviation Week & Space Technology*, Vol. 156 No. 25, pp. 62-62.

Bishop, C.M. (1995), *Neural Networks for Pattern Recognition*, Oxford University Press, New York, NY.

Brischetto, S. (2018), "Analysis of natural fibre composites for aerospace structures", *Aircraft Engineering and Aerospace Technology*, Vol. 90 No. 9, pp. 1372-1384.

Buhmann, M.D. (2003), *Radial Basis Functions: Theory and Implementations*, Cambridge University Press, New York, NY.

Daniel, I.M. and Ishai, O. (2006), *Engineering Mechanics of Composite Materials*, 2nd ed., Oxford University Press, New York, NY.

Davis, R.L. (2015), "Mechanical design and optimization of Swarm-Capable UAV launch systems", MSc thesis, Naval Postgraduate School, Monterey, CA.

Elmarakbi, A. (2013), *Advanced Composite Materials for Automotive Applications: Structural Integrity and Crashworthiness*, John Wiley & Sons, West Sussex.

Fernández-Godino, M.G., Balachandar, S. and Haftka, R.T. (2019), "On the use of symmetries in building surrogate models", *Journal of Mechanical Design*, Vol. 141 No. 6.

Glaz, B., Goel, T., Liu, L., Friedmann, P.P. and Haftka, R.T. (2009), "Multiple-surrogate approach to helicopter rotor blade vibration reduction", *AIAA Journal*, Vol. 47 No. 1, pp. 271-282.

Hao, P., Feng, S., Zhang, K., Li, Z., Wang, B. and Li, G. (2018), "Adaptive gradient-enhanced kriging model for variable-stiffness composite panels using isogeometric analysis", *Structural and Multidisciplinary Optimization*, Vol. 58 No. 1, pp. 1-16.

Hao, P., Feng, S., Li, Y., Wang, B. and Chen, H. (2020), "Adaptive infill sampling criterion for multi-fidelity gradient-enhanced kriging model", *Structural and Multidisciplinary Optimization*, Vol. 62 No. 1, pp. 353-373.

Hardle, W. (1990), *Applied Nonparametric Regression*, Cambridge University Press, Cambridge.

Holmes, M. (2017), "Aerospace looks to composites for solutions", *Reinforced Plastics*, Vol. 61 No. 4, pp. 237-241.

Myers, R.H. and Montgomery, D. (1995), *Response Surface Methodology: Process and Product Optimization Using Designed Experiments*, Wiley, Toronto.

Okpara, U. and Bier, V.M. (2008), "Securing passenger aircraft from the threat of man-portable air defense systems (MANPADS)", *Risk Analysis*, Vol. 28 No. 6, pp. 1583-1599.

Queipo, N.V., Haftka, R.T., Shyy, W., Goel, T., Vaidyanathan, R. and Tucker, P.K. (2005), "Surrogate-based analysis and optimization", *Progress in Aerospace Sciences*, Vol. 41 No. 1, pp. 1-28.

Sharma, A., Bhandari, R., Aherwar, A. and Rimašauskienė, R. (2019), "Matrix materials used in composites: a comprehensive study", *Materials Today: Proceedings*, Vol. 21, pp. 1559-1562.

Simon, A.J. (2006), "Raytheon aircraft protection systems", *Proceedings of SPIE, International Society for Optical Engineering*, p. 62030D-1.

Tempelman, E., Sherclif, H. and Eyben, N. (2014), *Manufacturing and Design: Understanding the Principles of How Things Are Made*, Elsevier, New York, NY.

Vasiliev, V.V. and Morozov, E.V. (2013), "Mechanics of a unidirectional ply", in Vasiliev, V.V. and Morozov, E.V. (Eds), *Advanced Mechanics of Composite Materials*, Elsevier, New York, NY, pp. 53-124.

Wagenen, R.V. (1989), A Guide to Structural Factors for Advanced Composites Used on Spacecraft, NASA Contractor Report 186010, Washington, DC.

Wang, W.T., Wu, J.H. and Kam, T.Y. (1999), "Design of a frangible laminated composite launch tube closure", *ASME International Mechanical Engineering Congress and Exposition, November 14-19, Nashville, TN*, pp. 129-138.

Yeh, H.Y., Murphy, H.C. and Yeh, H.L. (2009), "An investigation of failure criterion for new orthotropic ceramic matrix composite materials", *Journal of Reinforced Plastics and Composites*, Vol. 28 No. 4, pp. 441-459.

Appendix 1. Training points generated

In this study, Latin hypercube sampling is used to generate the training points. Tables A1 to A3 presents the training points generated for glass/epoxy, carbon/epoxy and aramid/epoxy, respectively.

Table A1 Training points for glass/epoxy material

Sample #	θ (°)	t_1 (mm)	t_2 (mm)	Weight (kg)	SF
1	1.67	1.05	1.61	3.66	5.57
2	5.00	0.56	0.14	1.23	1.41
3	8.33	1.26	1.54	4.00	5.46
4	11.67	0.21	1.40	1.79	2.36
5	15.00	1.96	0.35	4.21	5.44
6	18.33	0.98	1.05	2.96	4.52
7	21.67	0.77	1.75	3.24	5.29
8	25.00	1.33	1.96	4.56	5.68
9	28.33	1.47	1.47	4.35	5.80
10	31.67	0.28	1.19	1.72	2.48
11	35.00	1.75	0.49	3.93	5.85
12	38.33	0.70	0.56	1.92	2.91
13	41.67	1.82	0.70	4.28	6.06
14	45.00	0.63	0.21	1.44	1.94
15	48.33	1.61	0.42	3.59	6.33
16	51.67	0.84	0.84	2.48	4.84
17	55.00	0.91	1.89	3.66	8.55
18	58.33	1.12	1.26	3.45	8.37
19	61.67	0.14	0.28	0.54	0.56
20	65.00	1.19	1.82	4.14	9.20
21	68.33	1.54	1.33	4.35	8.43
22	71.67	0.42	0.63	1.44	3.28
23	75.00	1.40	0.91	3.66	8.36
24	78.33	1.89	0.77	4.49	7.33
25	81.67	1.68	1.12	4.42	8.24
26	85.00	0.35	0.98	1.65	5.31
27	88.33	0.49	1.68	2.62	11.79

Table A2 Training points for carbon/epoxy material

Sample #	θ (°)	t_1 (mm)	t_2 (mm)	Weight (kg)	SF
1	1.67	0.28	1.40	1.56	2.14
2	5.00	1.40	0.35	2.52	3.68
3	8.33	1.19	0.77	2.52	3.73
4	11.67	0.98	1.89	3.08	4.86
5	15.00	0.63	1.61	2.30	3.50
6	18.33	1.68	1.96	4.27	7.34
7	21.67	0.14	0.21	0.38	0.44
8	25.00	0.21	1.05	1.17	1.70
9	28.33	0.56	0.91	1.62	2.59
10	31.67	1.75	0.56	3.25	5.22
11	35.00	0.84	1.19	2.30	4.03
12	38.33	1.89	1.26	4.04	7.37
13	41.67	1.05	0.49	2.07	3.55
14	45.00	1.61	0.14	2.69	4.13
15	48.33	1.26	1.33	3.08	6.48
16	51.67	1.82	1.47	4.10	9.24
17	55.00	1.54	0.28	2.69	5.13
18	58.33	1.96	0.63	3.65	8.33
19	61.67	0.91	1.68	2.80	7.67
20	65.00	1.47	0.70	2.91	7.85
21	68.33	1.33	1.54	3.36	10.47
22	71.67	0.42	1.12	1.56	5.13
23	75.00	1.12	1.82	3.25	12.27
24	78.33	0.49	0.84	1.45	5.53
25	81.67	0.70	0.98	1.90	8.14
26	85.00	0.77	1.75	2.63	13.73
27	88.33	0.35	0.42	0.89	4.26

Table A3 Training points for aramid/epoxy material

Sample #	θ (°)	t_1 (mm)	t_2 (mm)	Weight (kg)	SF
1	1.67	0.28	1.40	1.37	0.98
2	5.00	1.40	0.35	2.21	0.95
3	8.33	1.19	0.77	2.21	0.95
4	11.67	0.98	1.89	2.70	0.90
5	15.00	0.63	1.61	2.01	0.96
6	18.33	1.68	1.96	3.73	0.87
7	21.67	0.14	0.21	0.33	0.17
8	25.00	0.21	1.05	1.02	0.76
9	28.33	0.56	0.91	1.42	0.93
10	31.67	1.75	0.56	2.85	0.90
11	35.00	0.84	1.19	2.01	0.93
12	38.33	1.89	1.26	3.54	0.90
13	41.67	1.05	0.49	1.81	0.95
14	45.00	1.61	0.14	2.35	0.95
15	48.33	1.26	1.33	2.70	1.03
16	51.67	1.82	1.47	3.58	1.08
17	55.00	1.54	0.28	2.35	1.03
18	58.33	1.96	0.63	3.19	1.13
19	61.67	0.91	1.68	2.45	1.59
20	65.00	1.47	0.70	2.55	1.43
21	68.33	1.33	1.54	2.94	2.15
22	71.67	0.42	1.12	1.37	2.38
23	75.00	1.12	1.82	2.85	3.91
24	78.33	0.49	0.84	1.27	3.61
25	81.67	0.70	0.98	1.66	4.30
26	85.00	0.77	1.75	2.30	5.31
27	88.33	0.35	0.42	0.78	2.41

Appendix 2. Surrogate models used

A brief overview of surrogate models is provided in the followings.

Polynomial response surface method

Polynomial response surfaces provide the relationship between design variables and the desired response by fitting a polynomial. The most commonly used polynomial response surface model is a quadratic polynomial, and it is expressed in equation (B.1):

$$\hat{y}(x) = b_0 + \sum_{i=1}^{L} b_i x_i + \sum_{i=1}^{L} b_{ii} x_i^2 + \sum_{i=1}^{L-1} \sum_{j=i+1}^{L} b_{ij} x_i x_j \tag{B.1}$$

where $\hat{y}$ is estimated function, x is design variables, L is the number of design variables and b values are the coefficients to be calculated while creating the model (Myers and Montgomery, 1995)

Kriging

In Kriging method, the response function is estimated by a formula consisting of two components as in equation (B.2):

$$y(x) = f(x) + Z(x) \tag{B.2}$$

where $f(x)$ is the polynomial function that converges globally to the response, and $Z(x)$ is the stochastic process with Gaussian distribution, with a mean of zero and a variance of σ^2, and can be called systematic deviation (Acar, 2013). The convergence matrix of $Z(x)$ is given in equation (B.3):

$$Cov\left[Z(x^i), Z(x^j)\right] = \sigma^2 R\left(\left[r(x^i, x^j)\right]\right) \tag{B.3}$$

where σ^2 variance refers to the $N \times N$ correlation matrix formed from N sampling points in R. $r(x^i, x^j)$ is the correlation function between the two sampling points x_k^i and x_k^j.

Nonparametric regression

Nonparametric regression provides improved response quality and is applied as a metamodeling technique for high nonlinear behavior of outputs relative to inputs. Nonparametric regression belongs to a general class of techniques of the support vector method (Hardle, 1990). These are data classification methods that use hyperplanes to separate groups of data. The regression method works similarly. The main difference is that the hyperplane is used to categorize a subset of input sample vector.

Let's assume that each x_i is an N-dimensional vector when we set the input sample as $X = \{x_1, x_2, x_3, \ldots, x_m\}$. The purpose is to determine the equation form specified in equation (B.4):

$$Y = \langle W, X \rangle + b \tag{B.4}$$

where W represents the weight vector. The expression specified in equation (B.4) can be written as in equation (B.5) in general non-parametric cases:

$$Y = \sum_{i=1}^{N} (A_i - A_i^*) K\left(\vec{X}_i, \vec{X}\right) + b \tag{B.5}$$

Here, $K(\ldots)$ is kernel function, A_i and A_i^* are Lagrange multipliers. The value of b is used as a constant. Starting with the assumption that the weight vector W must be minimized such that all (or most) of the sample points remain within an error zone, Lagrange multipliers are determined. The b value is obtained by applying Karush–Kuhn–Tucker conditions in the formulation created while determining Lagrange multiplier.

Figure A1 Neural network system

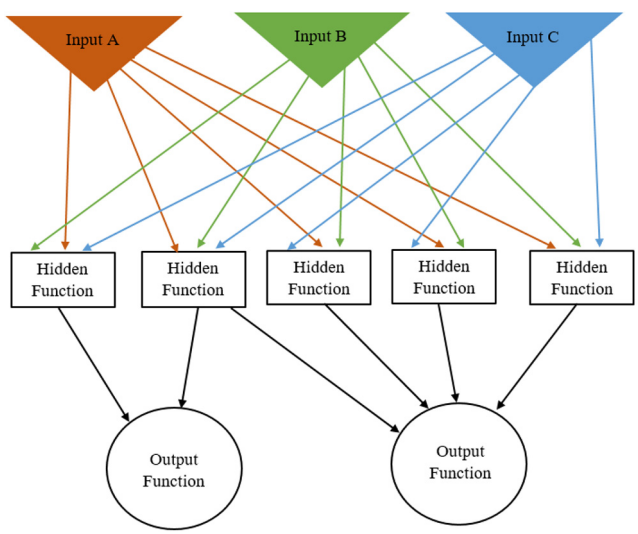

Table A4 Randomly selected test points for error metric

Glass/Epoxy			Carbon/Epoxy			Aramid/Epoxy		
t_1 (mm)	t_2 (mm)	θ (°)	t_1 (mm)	t_2 (mm)	θ (°)	t_1 (mm)	t_2 (mm)	θ (°)
0.11	0.12	86.09	1.95	0.63	0.48	1.99	1.99	89.33
1.06	0.10	1.75	1.97	1.88	0.30	0.11	2.00	47.35
0.15	1.97	65.94	0.14	1.45	29.45	1.98	1.14	89.31
1.42	1.06	1.14	0.69	0.38	89.36	1.95	0.12	89.49
1.99	0.32	50.85	0.18	0.10	20.34	1.94	1.03	0.92
1.98	1.31	25.76	1.71	1.99	60.06	1.15	0.13	86.76
1.99	0.69	88.23	1.08	1.90	88.83	0.35	0.12	55.69
0.16	1.15	51.64	0.87	0.18	48.61	0.73	0.12	2.87
0.90	1.93	1.17	1.02	1.15	89.30	0.11	1.98	81.21
1.77	1.96	41.40	0.28	0.75	39.62	1.45	1.46	1.27

Genetic aggregation

Genetic aggregation is a method based on using the weighted average of different surrogate models (Acar and Rais-Rohani, 2009). In this way, it automates the process of selecting, configuring, and generating the appropriate response surface type for each output parameter in the optimization problem. Genetic aggregation can be written as in equation (B.6) by using the weighted average of different meta models:

$$\hat{y}_{ens}(x) = \sum_{i=1}^{N_M} w_i.\hat{y}_i(x) \tag{B.6}$$

In equation (B.6), $\hat{y}_{ens}$ is the estimation of the group, $\hat{y}_i$ is the estimation of the i'th response, N_M is the number of metamodels and w_i is the weight factor of the i'th response surface. Weight factors must meet the conditions specified in equation (B.7):

$$\sum_{i=1}^{N_M} w_i = 1 \ \ and \ \ w_i \geq 0, \ \ 1 \leq i \leq N_M \tag{B.7}$$

Neural network

Neural network is a mathematical technique based on the natural neural network in the human brain (Bishop, 1995). To interpolate a function, often a three-level (input, hidden and output) network is created and the links between them are weighted. Figure A1 contains an exemplary neural network system.

Each arrow shown in Figure A1 is associated with a weight (w). Let the inputs contain x_i and the hidden level contain the function $g_j(x_i)$. In this case, the output solution is given in equation (B.8):

$$f_k(x_i) = K\left(\sum w_{jk} g_j(x_i)\right) \tag{B.8}$$

Here K is a predefined function, derived from an algorithm that minimizes the distance between weight functions (w_{jk}), interpolation, and known values (design points). This is called learning. When the error is the lowest, the error reduction algorithm is stopped.

Appendix 3. Randomly selected test points for error metric

As noted in the main text, the accuracies of the constructed surrogate models are evaluated at some randomly selected ten test points. These test points are provided in Table A4.

Corresponding author

Erdem Acar can be contacted at: acar@etu.edu.tr